Double-target Antisense U1snRNAs Correct Mis-splicing Due to c.639+861C>T and c.639+919G>A *GLA* Deep Intronic Mutations

Lorenzo Ferri[1,2], Giuseppina Covello[3], Anna Caciotti[2], Renzo Guerrini[1,2], Michela Alessandra Denti[3] and Amelia Morrone[1,2]

Fabry disease is a rare X-linked lysosomal storage disorder caused by deficiency of the α-galactosidase A (α-Gal A) enzyme, which is encoded by the *GLA* gene. *GLA* transcription in humans produces a major mRNA encoding α-Gal A and a minor mRNA of unknown function, which retains a 57-nucleotide-long cryptic exon between exons 4 and 5, bearing a premature termination codon. NM_000169.2:c.639+861C>T and NM_000169.2:c.639+919G>A *GLA* deep intronic mutations have been described to cause Fabry disease by inducing overexpression of the alternatively spliced mRNA, along with a dramatic decrease in the major one. Here, we built a wild-type *GLA* minigene and two minigenes that carry mutations c.639+861C>T and c.639+919G>A. Once transfected into cells, the minigenes recapitulate the molecular patterns observed in patients, at the mRNA, protein, and enzymatic level. We constructed a set of specific double-target U1asRNAs to correct c.639+861C>T and c.639+919G>A *GLA* mutations. Efficacy of U1asRNAs in inducing the skipping of the cryptic exon was evaluated upon their transient co-transfection with the minigenes in COS-1 cells, by real-time polymerase chain reaction (PCR), western blot analysis, and α-Gal A enzyme assay. We identified a set of U1asRNAs that efficiently restored α-Gal A enzyme activity and the correct splicing pathways in reporter minigenes. We also identified a unique U1asRNA correcting both mutations as effiently as the mutation-specific U1asRNAs. Our study proves that an exon skipping-based approach recovering α-Gal A activity in the c.639+861C>T and c.639+919G>A *GLA* mutations is active.

Introduction

Fabry disease (FD; OMIM 301500) is a rare X-linked lysosomal storage disorder caused by the deficiency of the lysosomal enzyme α-galactosidase A (α-Gal A; EC 3.2.1.22) which is encoded by the *GLA* gene (OMIM 300644, RefSeq NM_000169.2).[1] The prevalence of FD worldwide is estimated at 1/40,000–1/117,000.[1] Phenotypic expression of FD is highly variable,[2] ranging from a milder phenotype with cardiac and/or renal abnormalities, to classic FD, featuring, in addition to cardiac vascular degeneration, chronic pain, angiokeratoma, and kidney manifestations usually leading to renal failure.[2] Although FD is X-linked, heterozygous females may develop mild to severe clinical manifestations.[1–3]

The *GLA* gene transcribes two alternatively spliced mRNAs of which the most abundant (to which we refer as the "α-Gal A transcript") encodes the lysosomal α-Gal A. The minor mRNA (to which we refer as the "GLAins57") accounts for about 5% of total *GLA* transcripts.[4,5] GLAins57 retains a 57-nucleotide-long cryptic exon from intron 4 and is predicted to code for a shorter protein of unknown function.[5] An unbalanced expression of these two transcripts due to NM_000169.2:c.639+861C>T (g.9273C>T or IVS4+861C>T) and NM_000169.2:c.639+919G>A

(g.9331G>A or IVS4+919G>A) *GLA* deep intronic mutations has been reported to cause FD.[4,5] The c.639+861C>T mutation was associated with the classic FD phenotype in an Italian family.[4] The c.639+919G>A mutation is predominantly associated with late-onset FD[5,6] and is highly prevalent in Taiwanese newborns (1 in 1,600 males[7]; approximately 82–86% of positives[7,8]).

The therapeutic skipping of specific exons ("exon skipping") can be obtained by antisense oligonucleotides (AONs) annealing with splice junctions or exonic splicing enhancers (ESEs).[9–12] AONs have been used against several genes associated with disease to restore correct splicing or the open reading frame through selective removal of the mutated exon.[13] This strategy has been used in the treatment of Duchenne muscular dystrophy (DMD).[14] AONs have also been successfully applied to the *in vitro* correction of aberrant splicing events caused by mutations which activated cryptic splice sites in several genetic diseases, such as Leber congenital amaurosis, propionic and methylmalonic acidemia, ataxia telangiectasia, congenital disorders of glycosylation, Niemann-Pick disease type C, neurofibromatosis type 1 and 2, megalencephalic leukoencephalopathy with subcortical cysts type 1 or Pelizaeus-Merzbacher disease (reviewed in refs. 10,11).

It is vital that antisense molecules, when delivered to the cells, accumulate in the nucleoplasmic compartment where mRNA is synthesized and spliced. To improve localization efficacy, the antisense sequences can be inserted into one of the nuclear U small nuclear RNAs (UsnRNA).[15–17] The advantage of using antisense-RNAs (asRNAs) as therapeutic agents is that they are very specific and not immunogenic[16]; as yet no undesired activity for asRNAs has been reported.[10]

The therapeutic benefits of AONs are time-limited, and repeated administration is necessary. The use of asRNAs offers a major advantage as they can be delivered *in vivo* within expression cassettes as in conventional gene replacement therapies.[15–17] It is possible to transduce or transfect target cells using viral or nonviral delivery systems, leading to the production of asRNAs exploiting endogenous transcription.

At present, two classes of UsnRNAs have been successfully modified to modulate splicing: U1 snRNA[16] and U7 snRNA.[18,19] U1 snRNA recognizes the 5' splice site and mediates the first step of spliceosome assembly,[20] while U7 snRNA has a role in the processing of the 3' end of histone mRNA.[21]

U1snRNA promoter has been shown to be useful for the stable expression of antisense molecules and other therapeutic RNAs.[16,22] Eight nucleotides at the single-stranded 5' terminus of U1 can be replaced by unrelated sequences with up to 50 nucleotides, without affecting either stability or the ability to assemble into snRNP particles.[16,22] The U1snRNA and U7snRNA expression cassettes are small (about 600 bp), they work efficiently both in *in vitro* systems and in animals and can be delivered as part of lentiviral[23–26] or AAV vectors.[27–31]

We focus on the development of antisense U1snRNAs (U1asRNAs), designed to restore α-Gal A levels in the c.639+861C>T and c.639+919G>A *GLA* deep intronic mutations. Three different antisense constructs were tested for exon skipping activity in COS-1 cells transfected with *GLA* minigenes. U1asRNAs constructs were designed to target both the 3' and the 5' splice site of the *GLA* cryptic exon and differed by one nucleotide corresponding to the position complementary to the nucleotide mutated in the *GLA* pre-mRNA.

Our results indicate that a single U1asRNA molecule can be used to correct different mutations.

Results
Reporter minigenes replicate the unbalanced expression of *GLA* transcripts observed in patients
We and other authors[4,5] have shown that the *GLA* gene transcribes two alternatively spliced mRNAs: the major *GLA* mRNA "α-Gal A transcript" and the minor transcript "GLAins57".[4] *GLA* deep intronic mutations c.639+861C>T and c.639+919G>A cause FD by increasing the inclusion of the cryptic exon to around 85 or 70% of the total transcripts.[4,5]

To replicate the splicing process of the cryptic exon, we constructed a minigene in which the entire 1,718-bp-long sequence of *GLA* intron 4 was inserted into *GLA* cDNA between exons 4 and 5 (**Figure 1a**). This wild-type splicing reporter minigene, which we named WT minigene, carries a SV40 early region polyadenylation site and expresses the

GLA mRNA under the transcriptional control of the CMV promoter (**Figure 1a**). Upon transfection in COS-1 cells, the WT minigene produced a shorter, more abundant mRNA, and a longer mRNA, as assessed by semiquantitative Reverse Transcriptase-PCR (PCR) and by real-time PCR (**Figure 2a** and **Table 1**). We confirmed both amplicons by direct sequencing: the shorter band corresponded to the α-Gal A mRNA, while the longer to the GLAins57 mRNA harboring the inclusion of the 57 nt cryptic exon, as expected.

We subsequently constructed the splicing reporter minigenes for the c.639+861C>T and c.639+919G>A intronic mutations which we named c.639+861C>T minigene and c.639+919G>A minigene, respectively. When transfected into COS-1 cells, the GLAins57/total *GLA*mRNAs ratio was 40% for WT minigene, as revealed by quantitative real-time PCR. This ratio markedly increased for mutated minigenes: 95% for the c.639+861C>T minigene and 88% for the c.639+919G>A minigene (**Table 1**). Such data confirm that c.639+861C>T and c.639+919G>A mutations unbalance the expression of the *GLA* mRNAs causing an increment in the production of the *GLA* alternatively spliced mRNA.

Our real-time PCR probes are specific for the sequence of human *GLA* transcripts and did not yield any amplification when tested on nontransfected COS-1 cells (data not shown). Therefore, our quantitative data are not affected by the endogenous *GLA* expression of COS-1 cells.

Antisense U1asRNAs induce skipping of *GLA* cryptic exon
In order to induce skipping of the cryptic exon, we designed and produced four antisense constructs, in the backbone of the U1 snRNA, and named them U1-GLAWT, U1-GLA3T, U1-GLA5A, and U1-GLAScramble. Nucleotides from position 3–10 at the 5′-end of U1 snRNA, required for the recognition of the 5′ splice site, were substituted with 48-nt-long antisense sequences complementary to both cryptic 3' and 5' splice sites (**Figure 1a**,**b**). The use of double-target U1asRNAs was dictated by indications in the literature demonstrating that efficient exon skipping is obtained with antisense U7 snRNAs[19] and antisense U1snRNAs[24,27–29,31] targeting at the same time two distinct splicing-regulating regions.

The chimeric U1-antisense sequences were cloned under the control of the strong RNA polymerase II U1 snRNA gene promoter and termination sequences and subsequently inserted into the pAAV2.1-CMV-EGFP plasmid.[32]

Construct U1-GLAWT produces a U1asRNA complementary to the cryptic splice sites of the wild-type *GLA* gene (**Figure 1b**), while constructs U1-GLA3T and U1-GLA5A differ from U1-GLAWT each by one nucleotide, being perfectly complementary to the 3' splice site of mutation c.639+861C>T and to the 5' splice site of mutation c.639+919G>A, respectively.

As a negative control, we also produced the U1-GLAScramble construct that bears a 23-nt-long sequence (**Figure 1b**) with no known target in mammalian cells.

U1-GLA5A, U1-GLA3T, and U1-GLAWT antisense constructs did not induce any significant variation on the *GLA* mRNA expression level when cotransfected with the wild-type minigene (**Figure 2a**).

Cotransfection analysis of U1-GLA3T and U1-GLAWT partially restored the expression of the α-Gal A mRNA in the presence of the c.639+861C>T mutation (**Figure 2b**) and
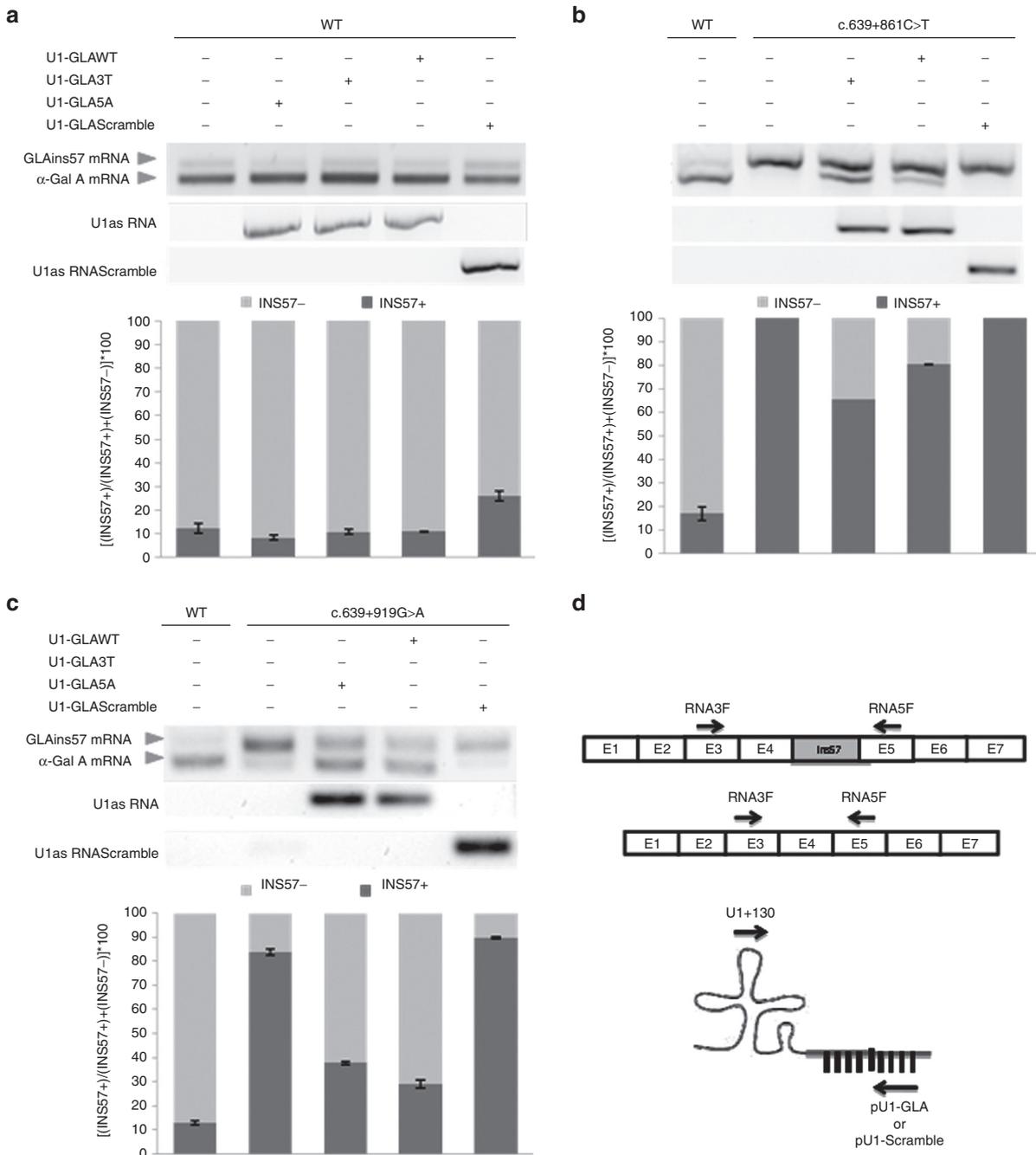
Figure 1 Experimental strategy adopted in this work. (**a**) Schematic representation of *GLA* splicing reporter minigene. (**b**) Antisense sequences used in this study. (**c**) Schematic representation of the exon-skipping strategy for the *GLA* cryptic exon.

U1-GLA5A and U1-GLAWT corrected, albeit not completely, the c.639+919G>A mutation (**Figure 2c**). These results indicate that the U1-GLAWT construct induces skipping of the cryptic exon in both c.639+861C>T and c.639+919G>A *GLA* mutations with a reduction of the GLAins57 mRNA of 66% for the c.639+861C>T and 20% for the c.639+919G>A, relative to cells transfected with the minigene alone (**Figure 2**). The control U1-GLAScramble did not cause any considerable alteration to the expression profile of any minigene, as expected (**Figure 2**).

Because the different antisense constructs considerably extend the length of the U1 snRNA (by 40 nucleotides), we checked the integrity of the U1 antisense RNAs and compared their levels in cotransfected COS-1 cells. We performed semiquantitative RT-PCR analyses with a primer annealing to the 5' variable tail and a primer annealing to a common portion of the U1 snRNA (**Figure 2d**). A specific amplification product of the expected size (around 100 bp) was obtained exclusively in the cells transfected with one of the U1asRNA constructs, confirming that they were produced in their entire length at comparable levels (**Figure 2**).

In order to assess the efficiency of exon skipping, we performed quantitative analyses of mRNA products from the *GLA* minigenes by absolute real-time PCR. To determine the absolute quantities of the two products, we used pCD-GLA vector and the oligonucleotide *GLA*mut to generate the standard curves. We analyzed total RNA isolated from the transfected COS-1 cells with *GLA* minigenes alone or in combination with U1asRNAs. Results are shown in **Table 1**.

Relative to the level of expression of α-Gal A mRNA in cells transfected with the WT minigene (100%), cells transfected with the c.639+861C>T minigene expressed 46.3% less the α-Gal A mRNA and 1323.9% more the GLAins57 mRNA, while cells transfected with the c.639+919G>A minigene expressed 57.1% less the α-Gal A mRNA and 633% more the GLAins57 mRNA (**Table 1**).

Administration of the U1-GLA3T to the c.639+861C>T minigene enhanced the expression of the α-Gal A mRNA by 150.7% and reduced the expression of the GLAins57 mRNA by 66.8% (**Table 1**).

Administration of the U1-GLA5A to the c.639+919G>A minigene enhanced the expression of the α-Gal A mRNA by 166.7% and reduced the expression of the GLAins57 mRNA by 41.6% (**Table 1**).

The cotransfection of the c.639+861C>T or the c.639+919G>A minigenes with the U1-GLAWT enhanced the expression of the α-Gal A mRNA by 141.8 and 166.7%, respectively; while it reduced the expression of the GLAins57 mRNA by 64.8 and 37.2%, respectively (**Table 1**).

Cotransfection of both minigenes with the U1-GLA Scramble had no influence on the transcripts levels, as expected (**Table 1**).

Figure 2 Screening of specific U1asRNA by RT-PCR analysis. Splicing assay and densitometric analysis of semiquantitative RT-PCRs of (**a**) wild-type, (**b**) c.639+861C>T, (**c**) c.639+919G>A minigenes transfected with or without the U1asRNAs. RT-PCR analysis of transcripts from U1-GLA5T, U1-GLA3A, U1-GLAWT (middle panel) and U1-GLAScramble (lower panel) were shown. (**d**) Schematic representation of both reporter *GLA* minigene cassette and chimeric U1 snRNAs. Arrows represent primer (not to scale). Data are expressed as mean (± standard deviation) of two independent experiments.

The results show that the U1-GLAWT construct is as efficient as the mutation-specific U1asRNAs, indicating that one mismatch in the 48-nt long antisense sequence is well tolerated. These data could have important implications as the same antisense molecule could be used to correct different mutations, without the need for personalized therapeutic molecules.

Antisense U1asRNAs increase α-Gal A protein levels

We performed immunoblot analyses to evaluate α-Gal A protein levels in transfected COS-1 cells. A reduced amount of α-Gal A protein was detectable in COS-1 cells transfected with c.639+861C>T (**Figure 3a**) or c.639+919G>A (**Figure 3b**) minigenes, with respect to cells transfected with wild-type minigene. These results

Table 1 Number of α-Gal A mRNA and GLAins57 mRNA copies detected by real-time PCR in COS-1 cells transiently transfected with *GLA* reporter minigenes and U1asRNA constructs

Minigene	Number of α-Gal A mRNA copies ± SD*	Percentage of α-Gal A mRNA copies with respect to the wild-type	Relative increase**	Number of GLAins57 copies ± SD*	Percentage of GLAins57 mRNA copies with respect to the wild-type	Relative decrease**
Wild-type	3.15E+08±4.72E+07	100%	–	2.13E+08±2.07E+07	100%	–
c.639+861C>T	1.46E+08±9.20E+06	46.3%	–	2.82E+09±5.63E+08	1,323.9%	–
c.639+861C>T + U1-GLA3T	2.20E+08±9.03E+06	69.8%	150.7%	9.35E+08±4.63E+08	439%	66.8%
c.639+861C>T + U1-GLAWT	2.07E+08±1.07E+07	65.3%	141.8%	9.91E+08±5.36E+08	465.2%	64.8%
c.639+861C>T + U1-GLAScramble	1.39E+08±3.90E+07	44.1%	95%	2.51E+09±3.73E+08	1,178.4%	11%
c.639+919G>A	1.80E+08±1.34E+07	57.1%	–	1.35E+09±2.00E+08	633%	–
c.639+919G>A + U1-GLA5A	3.00E+08±1.44E+07	95.2%	166.7%	7.88E+08±6.97E+07	369.9%	41.6%
c.639+919G>A + U1GLAWT	3.00E+08±5.97E+06	95.2%	166.7%	8.48E+08±2.65E+07	398.1%	37.2%
c.639+919G>A + U1-GLAScramble	1.73E+08±2.64E+07	54.9%	96.1%	1.25E+09±2.00E+08	586.8%	7.4%

*mean ± standard deviation calculated from three independent experiments. **with respect of the mutated minigene transfected without U1-asRNAs.
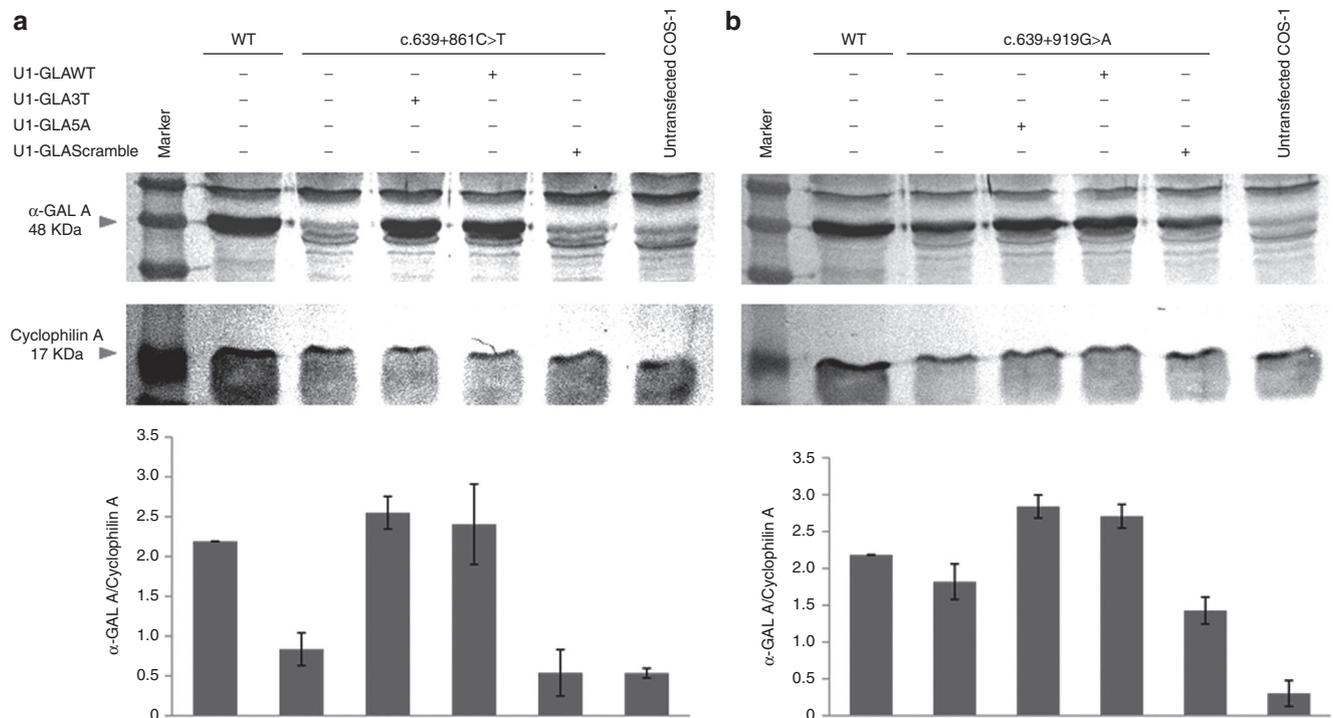
Figure 3 Western blot analysis of α-Gal A protein in transiently transfected COS-1 cells with (**a**) c.639+861C>T or (**b**) c.639+919G>A minigenes alone or in combination with specific U1asRNAs. Blots were carried out using 30 µg total protein with the anti-α-Gal A antibody (upper panels) and an anti-cyclophilin A antibody as a loading control (lower panels). The histograms represent the average amount (*n* = 2) of α-Gal A protein normalised over the amount of cyclophilin A protein, as assessed by densitometric quantification.

were consistent with what we observed at the level of *GLA* transcripts. The c.639+861C>T mutation reduced the expression of α-Gal A protein to a greater extent than the c.639+919G>A (**Figure 3**). Cotransfection of U1-GLA3T with the c.639+861C>T minigene as well as of U1-GLA5A with the c.639+919G>A minigene caused a significant increase in the α-Gal A protein detected by western blot (**Figure 3**). An increase in α-Gal A was also present when we cotransfected c.639+861C>T and c.639+919G>A minigenes with the U1-GLAWT (**Figure 3**). As expected, no differences in α-Gal A protein levels were detected when we cotransfected minigenes with the control U1-GLAScramble (**Figure 3**).

Antisense U1 snRNAs restore α-Gal A activity in c.639+861C>T and c.639+919G>A mutations

The α-Gal A basal activity of COS-1 cells was 103 ± 6.9 nmol/mg prot/hour (average of five independent replicates) and this amount was subtracted from the α-Gal A activities measured in the transfected cells. The α-Gal A enzyme activity of COS-1 cells transfected with wild-type minigene with respect to untransfected cells rose nearly 800% (816.2 ± 62.2 nmol/mg prot/hour, average of three independent replicates after subtraction of COS-1 basal α-Gal A activity). Residual α-Gal A activity was 5% of the wild-type for the c.639+861C>T mutation (**Figure 4b**) and 55% of the wild-type for the c.639+919G>A mutation (**Figure 4c**).
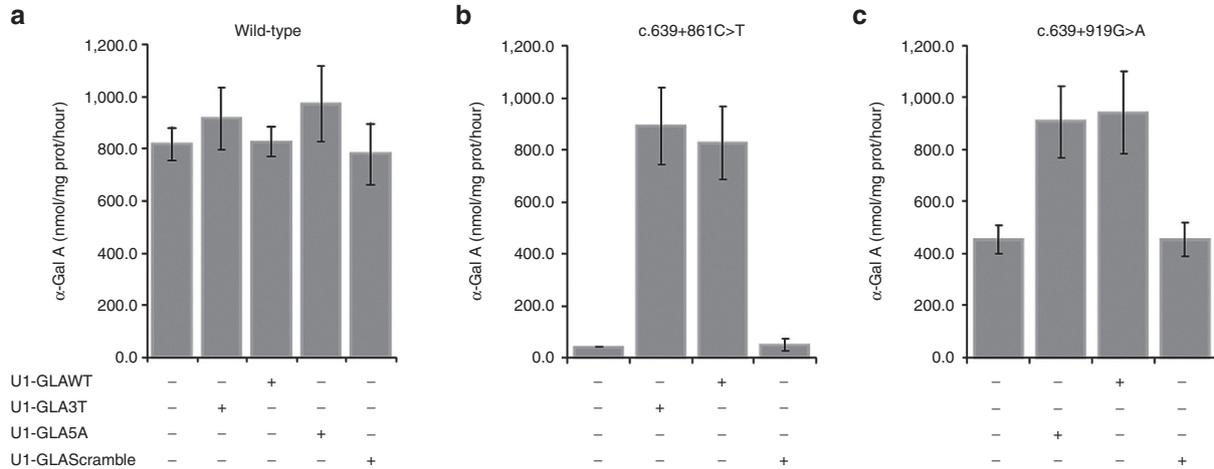
Figure 4 α-Gal A enzyme activities (expressed as nmol 4-MU released/mg protein/hour) in lysates that were prepared from transiently transfected COS-1 cells with minigenes: (**a**) c.639+861C>T, (**b**) c.936+919G>A and (**c**) wild-type with and without the supplementation of specific U1asRNAs. Data represent mean (± standard deviation) of three independent experiments ($P < 0.05$).

U1asRNAs were able to restore α-Gal A enzyme activity (**Figure 4**). In particular, U1-GLA3T and U1-GLAWT efficiently recovered enzyme activity in the mutation c.639+861C>T to levels equal to the wild-type (**Figure 4b**). Similarly, U1-GLA5A and U1-GLAWT efficiently restored the c.639+919G>A mutation. The U1-GLAScramble control did not perturb α-Gal A enzyme activity which resulted to be as low as in cells transfected with mutant minigenes alone (**Figure 4**).

When cotransfected with the wild-type minigene, none of the U1asRNAs significantly influenced α-Gal A enzyme activity (**Figure 4a**).

Discussion

Since 2001, enzyme replacement therapy (ERT) has been the only available specific treatment for FD.[33] ERT involves regular intravenous infusions of one of the two recombinant enzyme formulations available in Europe: agalsidase alfa (Replagal; Shire, Cambridge, MA), produced using cultured human skin fibroblasts and agalsidase beta (Fabrazyme; Genzyme, Cambridge, MA), produced by expressing human α-galactosidase cDNA in Chinese Hamster Ovary (CHO) cells. Published reports strongly support the overall clinical benefit of ERT, but benefits on renal and nervous system function are less obvious.[34–37] Some patients may develop a specific antibody response to the exogenous protein and, overall, therapy is very expensive.[38]

Pharmacological Chaperone Therapy (PCT) can offer an alternative approach. For some α-Gal A missense mutations the supplementation of pharmacological chaperone 1-deoxy-galactonojirimycin (DGJ or AT1001), an imminosugar with a structure resembling the α-galactose of globotriaosylceramide (Gb$_3$), improves endogenous α-Gal A activity.[39–41] Pharmacological Chaperone Therapy is currently being tested in clinical trials.[42,43]

A significant number of *GLA* disease-causing mutations are missense variants, which cause the newly synthesized lysosomal protein to be misfolded, but still catalytically competent.[44,45] The misfolded enzyme forms are unable to undergo appropriate trafficking to the lysosomal compartment and are prematurely degraded in the endoplasmic reticulum.[46] The active-site-specific chaperone DGJ stabilizes the conformation of the mutant proteins assisting protein folding and preventing premature degradation by Endoplasmic-reticulum-associated protein degradation (ERAD).[47,48] DGJ could provide additional advantages in terms of cost, whose use, however, would be limited to patients with specifically responsive *GLA* missense mutations.[49,50]

An attractive alternative approach aimed to correct RNA defects in human diseases is based on the exon skipping (ES) strategy. An interesting way to pursue ES is based on the use of antisense modified U snRNAs (such as U1 or U7) which can be delivered by adeno-associated viral vectors (AAV).[28–31,51–53]

ES based on virally-vectored modified U1 snRNAs offers the possibility of providing a long-term therapy which would only require a single administration in a patient's lifetime, by promoting stable genomic integration with viral delivery particles.[16] Modified U1 snRNAs have been shown to produce effective ES in several diseases.[10,11,14] Here, we have sought to evaluate U1-based ES for the correction of c.639+861C>T and c.639+919G>A mutations in FD.

We constructed a set of specific U1asRNAs and built *GLA* minigenes to express two deep intronic mutations, c.639+861C>T and c.639+919G>A.

Regulated alternative splicing is assumed to contribute to cell type identity. A different repertoire of splicing factors and other RNA-binding proteins is present in different cell types.[54] Additionally, it has been suggested that nucleosome density and histone modifications, which could also be cell-specific, may play a role in splice site recognition and regulation.[55] Nonetheless, cell-based splicing of minigenes, a simplified system, is used extensively for identifying or confirming the *in vivo* relevance of *cis-* and *trans-*acting factors in the regulation of particular splicing patterns.[56]

Although bioinformatic tools might be used to predict the effect of a nucleotide change on splicing, experimental

verification by minigenes is still required for diagnostic purposes, for revealing disease mechanisms and for monitoring therapeutic interventions.[57] The minigene-based analysis represents a complementary approach to reverse transcription-PCR analyses of patients' RNA, for the identification of pathogenic splicing.[58]

The exon carrying the mutation under study is cloned along with its flanking intronic sequence. The resulting construct, in its wild-type and mutant sequence version, is transfected in established cell lines, and the vector splicing pattern is analyzed. Ideally, the wild-type minigene results in correct exon inclusion, while the mutant construct results in aberrant transcripts. The splicing pattern observed when transfecting minigenes in different cell lines recapitulates the effect that a mutation has on the splicing of the different isoforms in patients' primary cells. However, in minigene studies, it is not unusual to observe a different ratio of correct vs. aberrantly spliced transcripts, with respect to patients' cells and from cell type to cell type. This might be likely due to the cell type-specific repertoires of splicing factors and RNA-binding proteins and to the fact that the minigene is a simplified system compared to the genomic DNA.

In this paper, we report the construction of a *GLA* wild-type minigene and two mutant *GLA* minigenes, harboring the mutations c.639+861C>T and c639+919G>A.

Upon transfection into COS-1 cells, the wild-type *GLA* minigene generated *GLA* transcripts of which 60% were α-Gal A mRNA and 40% were GLAins57, as assessed by real-time PCR. Our real-time PCR probes are specific for the human *GLA* sequence and did not yield any amplification when tested on non-transfected COS-1 cells (data not shown). Therefore, our real-time PCR data are not affected by the endogenous expression of the COS-1 *GLA* gene. The difference in the percentage of GLAins57 can be explained by the simplified nature of reporter minigenes systems, compared to the endogenous gene and the fact that COS-1 cells contain a different repertoire of splicing factors. However, our data are in line with the observations of Ishii and colleagues[5] that showed small amounts of GLAins57 transcripts (<10% of total *GLA*) in the kidney, spleen, and liver of normal individuals, and even higher amounts in muscle and lung tissues. Importantly, the mutated minigenes recapitulated the splicing pattern present in patients' cells. When transfected into COS-1 cells, the c.639+861C>T minigene gave rise to a higher number of GLAins57 transcripts (ca. ten-fold increase) and a lower number of α-Gal A mRNA (ca. three-fold decrease), when compared to the wild-type minigene. Similarly, the c.639+919G>A minigene caused a two-fold higher expression of the GLAins57 transcript and a five-fold decrease of α-Gal A mRNA, when compared to the wild-type minigene.

Importantly, the c.639+861C>T minigene led to a higher expression of the GLAins57 transcript and a lower residual α-Gal A activity than the c.639+919G>A minigene. Such results confirm what has been observed in Fabry patients, because the c.639+861C>T mutation is associated with a heavily α-Gal A enzyme deficiency in males and a more severe phenotype than the c.639+919G>A mutation.[5,40]

By testing U1asRNAs against the minigene systems, we identified three U1asRNAs with a marked splicing correction activity. The U1-GLA5T was able to restore full α-Gal A enzyme activity and protein for the c.639+861C>T mutation and a similar effect was obtained with U1-GLA3A for the c.639+919G>A mutation. The administration of U1-GLA3T or U1-GLAWT to the c.639+861C>T minigene, and of U1-GLA5A or U1-GLAWT to the c.639+919G>A minigene, significantly reduced the expression of the GLAins57 mRNA.

Results indicate that U1-GLA5A, U1-GLA3T, and U1-GLAWT antisense constructs are able to prevent the inclusion of the cryptic exon in the mutated minigenes with variable efficiencies, depending on the targeted sequence. The U1-GLAWT construct is able to prevent the inclusion of the cryptic exon in both the c.639+861C>T and c.639+919G>A mutations, indicating that one mismatch in the 48-nt long antisense sequence is well tolerated, as expected. In fact, U1-GLAWT would bind with a G:U wobble base pair in the 3'ss to the c.639+861T mutant pre-mRNA, compared to a G:C base pair present in the same position in the binding to the wild-type pre-mRNA. This translates in a difference in standard free energy of only about 1.5 Kcal/mol. However, U1-GLAWT would bind with a A/C mismatch the 5'ss of the c.639+919A mutant pre-mRNA, compared to a G:C base pair present in the same position in the binding to the wild-type. This translates into a difference in standard free energy of about 6 Kcal/mol. Hence, a single mismatch probably is not likely to abrogate the binding of the 48-nt long sequence to the target (which in the wild-type conditions is of about ΔG = −80 Kcal/mol). These data have important implications because a universal U1-based ES strategy could be used to correct different mutations affecting this specific alternative splicing process of the *GLA* gene.

The accumulation of globotriaosylceramide (Gb3) and related glycolipids in FD is progressive and occurs in fluids and tissues including vascular endothelium, kidney, heart, connective tissue, and peripheral nerves.[2,59] FD males who have little or no functional α-Gal A enzyme activity (<1% of normal mean) develop early accumulation of Gb3 in capillaries and small blood vessels which cause the major symptoms in childhood or adolescence (acroparesthesias; anhidrosis or hypohidrosis; angiokeratomas; gastrointestinal problems; corneal dystrophy).[2,59] With advancing age, the progressive Gb3 deposition leads to renal, heart, and cerebrovascular manifestations (transient ischemic attacks or strokes). End-stage renal disease and life-threatening cardiovascular or cerebrovascular complications limit life-expectance.[3,60,61]

Renal lesions result from Gb3 deposition in the glomerular endothelial, mesangial, interstitial cells, in podocytes, in the epithelium of the loop of Henle and the distal tubules, and in the endothelial and smooth muscle cells of the renal arterioles.[59] Gb3 deposition can be found in all cardiac tissues, including myocytes, nerves, and coronary arteries.[62] Cerebrovascular complications are a result of progressive Gb3 deposition in the small blood vessels in the brain.[2,59]

Interestingly, it has been reported that repeated infusions with ERT over a prolonged period did not appreciably clear storage material in cells other than vascular endothelial cells.[63,64] In the samples from the heart and some other tissues biopsied from two male patients after several months of ERT, only the endothelial cells were free of Gb3 and persistent storage was found in cardiomyocytes, smooth muscle

U1asRNAs-based mRNAs Correction in *GLA* Deep Intronic Mutations
Ferri et al.

8

cells, fibroblasts, and sweat glands.[63] Similarly, extensive glycolipid storage deposits were seen in all organ systems with the exception of vascular endothelial cells in the autopsy study of a 47-year-old male patient who died after 2.5 years of ERT with agalsidase-β.[64]

At variance with classical gene therapy approaches, splicing-modulating therapeutic approaches have the advantage of a great specificity of action, since they are based on nucleic acids base-pairing with their target RNA. Since they act at the pre-mRNA level, their effect is dependent on the transcriptional regulation of the target gene: the therapeutic effect is obtained only where and when the target pre-mRNA is present. Therefore, a tissue-specific therapeutic effect could be envisaged for the U1asRNA described in the present paper, if systemically delivered via AAV vectors.

U1asRNAs have been effectively and stably delivered through tail vein injection of AAV vectors with an AAV1 capsid, in a mouse model of Duchenne Muscular Dystrophy, showing good bio-distribution to liver, skeletal muscles, and heart.[27,29] More recently, alternative AAV vector serotypes have been implemented, such as AAV8 and AAV9, showing transduction in a broader range of tissues, including heart, liver, skeletal muscle, brain, kidney, and lung,[53,65] and higher efficiency of myocardial transduction in mice.[66,67] Intravenous injection of AAV9 resulted in persistent global central nervous system and broad somatic transduction in primates.[68] Intravenous injection of AAV8 has been tested in phase 2 clinical trials for the gene therapy of hemophilia B.[69] In the future, we might expect the availability of more specific AAV vectors, given the active research in the field of directed evolution of cell type-selective AAVs.[70]

Although the majority of the causative *GLA* gene mutations are private, the c.639+919G>A mutation is quite common in the Asian population.[7,8] On the other hand, the c.639+861C>T mutation was identified in one isolated Italian family. In particular, the c.639+919G>A mutation was found with a very high prevalence among newborns in Taiwan (1 in 1,600 males[7]; approximately 82–86% of patients carrying a *GLA* mutation).[7,8] If a specific antisense RNA-based drug to correct this mutation was made available, it could benefit a high number of Fabry patients. A U1asRNA-based therapy would act on the pre-mRNA endogenously produced in the affected cells, thus maintaining the physiological *GLA* gene transcription regulation. Since the c.639+919G>A mutation does not completely impair the α-Gal A protein production leading to residual enzyme activity,[5] we can hypothesize that a U1-based therapeutic approach would be well tolerated in patients without the development of an anti-α-Gal A immune response as occurring with ERT.[71] Anyhow, further experiments focused on patients' derived cell lines or animal models will be necessary to confirm such speculations.

Our study provides evidence that splicing correction through a U1-vectored antisense RNA could be developed to restore α-Gal A production and enzyme activity in the c.639+861C>T and c.639+919G>A *GLA* mutations. It will now be possible to proceed towards preclinical trials for this therapeutic approach, delivering the antisenseU1-producing cassette to patients' cells and animal models via viral vectors.

Materials and methods

Construction of GLA reporter minigenes. We constructed wild-type and mutated *GLA* minigenes for the expression of c.639+861C>T and c.639+919G>A mutations by integration of the full-length sequence of the human *GLA* intron 4 within the wild-type human *GLA* cDNA. We engineered the wild-type human *GLA* cDNA sequence that had previously been cloned in the pCD-X vector in our laboratory.[40] This plasmid (pCD-GLA) is suitable for expression in mammalian cells.[40]

The entire *GLA* intron 4 was amplified from human wild-type DNA or from a male patient's DNA harboring the c.639+861C>T *GLA* mutation. We used oligonucleotides cDNAcap4F and cDNAcap5R (**Table 2**) that anneal in exon 4 and exon 5, respectively. Two *GLA* cDNA fragments corresponding to exons 1–4 and exons 5–7 were amplified from pCD-GLA plasmid with primer pairs 5XBAGLA + cDNAcap4R and cDNAcap5F + 3ECOGLA. The obtained PCR fragments were mixed in separate mixtures with wild-type or c.639+861C>T *GLA* intron 4 and used as templates for a PCR reaction with external primers 5XBAGLA and 3ECOGLA to produce the minigene cassette. All the PCR amplifications were performed with high fidelity Platinum *Pfx* DNA polymerase (Thermo Fisher Scientific, Waltham, MA). The pCD-GLA plasmid and the minigene cassettes were cut with endonucleases XbaI and EcoRI (New England Biolabs, MA) that each recognize a unique restriction site. The digested fragments were linked using Solution I of the DNA Ligation Kit Ver.2.1 (TaKaRa Bio, Kusatsu, Japan) and cloned by transforming the *E. coli* Solopack gold cells (Agilent Technologies, Santa Clara, CA). The final constructs were checked by agarose gel electrophoresis and by sequencing. EndoFree Plasmid Maxi Kit (Qiagen, Hilden, Germany) was used to purify the plasmids, which were called WT minigene (with the wild-type *GLA* intron4) and c.639+861C>T minigene (with the c.639+861C>T mutation).

To introduce the Asian *GLA* c.639+919G>A mutation, for which patient-derived genomic DNA was not available, we used general procedures for site directed mutagenesis. The WT minigene was amplified by PCR with specific mutated oligonucleotide primers GLA919A-fw and GLA919A-rev, in combination with primers 3ECOGLA and 5XBAGLA. The obtained PCR fragments were mixed and used as templates for a PCR reaction with external oligonucleotides 5XBAGLA and 3ECOGLA to produce the minigene cassette. The pCD-GLA plasmid and the minigene cassette were cut with endonucleases XbaI and EcoRI (New England Biolabs). The final mutated construct was obtained by ligation and cloning and was verified by direct sequencing, as previously described. We called the obtained minigene c.639+919G>A minigene.

Production of antisense U1 snRNA constructs. We obtained plasmids U1-GLA3T, U1-GLA5A, U1-GLAWT and U1-GLAScramble by inverse PCR of the U1 snRNA genomic sequence, as described previously[29], using the oligonucleotides (Eurofins MWG Operon company, Ebersberg, Germany) reported in **Table 2**.

100 pmol of U1-GLA3CFOR, U1-GLA3TFOR, U1-GLA-5GREV, U1-GLA5AREV, U1-ScrambleRev primers were phosphorylated in a final volume of 100 µl by using T4 Polynucleotide kinase (Fermentas, Thermo Fisher Scientific),

Table 2 Oligonucleotides used in this study

Primer	Sequence
PCR primers	
cDNAcap4F	5′-GAAGCATTGTGTACTCCTGT-3′
cDNAcap5R	5′-CTGTCGGATTTCTGTATAAT-3′
5XBAGLA	5′-CTCTAGAATGCAGCTGAGGAA-3′
cDNAcap4R	5′-ACAGGAGTACACAATGCTTC-3′
cDNAcap5F	5′-ATTATACAGAAATCCGACAG-3′
3ECOGLA	5′-CCGAATTCTTAAAGTAAGTCTTTTAA-3′
GLA919A-fw	5′-TCCCCACTAAAGTGTAAGTT-3′
GLA919A-rev	5′-AACTTACACTTTAGTGGGGA-3′
RNA3F	5′-TTCACAGCAAAGGACTGAAG-3′
RNA5R	5′-TGGTCCAGCAACATCAACAA-3′
U1-GLA3CFOR	5′-CAAATAGTGTGGAGCTCTGA**G**AAGGGCAGGGGAGATACCATGATC-3′
U1-GLA3TFOR	5′-CAAATAGTGTGGAGCTCTGA**A**AAGGGCAGGGGAGATACCATGATC-3′
U1-GLA5GREV	5′-CCACTA**G**AGTGTAAGTTTCATGAGATGAGATCTTGGGCCTCTGC-3′
U1-GLA5AREV	5′-CCACTA**A**AGTGTAAGTTTCATGAGATGAGATCTTGGGCCTCTGC-3′
U1-ScrambleRev	5′-TCAATTATTCCGCGAGACGCAGCATGAGATCTTGGGCCTCTGC-3′
U1-casup-FORNheI	5′-CTAGCTAGCGGTAAGGACCAGCTTCTTTG-3′
U1-casdown-REVNheI	5′-CTAGCTAGCGGTTAGCGTACAGTCTAC-3′
U1-univ-NheI	5′-GGCAGGGGAGATACCATGATC-3′
AAVRev	5′-CCATATATGGGCTATGAATAATG-3′
U1+130	5′-AGCACATCCGGAGTGCAATG-3′
pU1-GLA	5′-CAAATAGTGTGGAGCTCTG-3′
pU1-Scramble	5′-CTGCGTCTCGCGGAATAATTG-3′
Real time probes and primers	
631/666 nt (VIC)	5′-TTTCAAAAGCCCAATTATACAGAAATCCGACAGTAC-3′
579/602 nt	5′-GACTGGCAGAAGCATTGTGTACTC-3′
688/668 nt	5′-CAAAATTTCGCCAGTGATTGC-3′
670/701 nt (FAM)	5′-CTTGTTACCATGTCTCCCCACTAAAGTCCCAA-3′
642/668 nt	5′-CTCCACACTATTTGGAAGTATTTGTTG-3′
738/718 nt	5′-TCGCCAGTGATTGCAGTACTG-3′

All PCR primers were purchased from Eurofins MWG Operon company, Ebersberg, Germany. Real-time probes and primers were purchased from Applied Biosystems by Life Technologies.

following the manufacturer's protocols. After incubation of 30 minutes at 37 °C, the reaction was stopped by the addition of 1 µl of EDTA 0.5 M pH 8.0. Oligonucleotides were purified by the adding 100 µl of chloroform and centrifuged for 2 minutes at 16,000 × g. The U1-GLA3T, U1-GLA5A, U1-GLAWT, and U1-Scramble fragments were obtained via two distinct inverse PCR amplifications, performed on the pBSU1 plasmid containing the U1 snRNA gene.[29] The following phosphorylated and non-phosphorylated primer couples were used for the first PCR amplification reaction: U1-GLA3CFOR and U1-casdown-REVNheI; U1-GLA3TFOR and U1-casdown-REVNheI; U1-GLA5GREV and U1-casup-FORNheI; U1-GLA5AREV and U1-casup-FORNheI; U1-ScrambleRev and U1-casup-FORNheI, U1-univ-NheI and U1-casdown-REVNheI. All the PCR amplifications were performed in a final volume of 50 µl in a reaction mixture containing 1× of Cloned *Pfu* DNA polymerase reaction buffer, 200 µmol/l dNTPmix, 0.2 µmol/l of each primer, 2U of Cloned *Pfu* DNA polymerase Taq (Agilent Technology, Santa Clara, CA). DNA was denatured for 1 minute at 95 °C, followed by 30 cycles of amplification with cycling conditions of 95 °C for 1 minute, 65 °C for 40 seconds, extension at 72 °C for 45 seconds, and extra final extension at 72 °C for 7 minutes.

Amplification products sizes are 215 bp for U1-GLA3C, U1-GLA3T, U1-univ fragments and 419 bp for U1-GLA5G, U1-GLA5A and U1-Scramble fragments. After PCR reactions all the products were extracted from a 1% agarose gel in Tris-Acetic Acid-EDTA (TAE) 1X (Sigma-Adrich, St. Louis, MO) using the *QIAquick Gel Extraction Kit* according to the manufacturer's protocol (Qiagen, Hilden, Germany), and the single fragments were ligated in order to obtain the whole U1-GLA3T, U1-GLA5A, U1-GLAWT, and U1-Scramble fragments. Ligation was performed in a final volume of 20 µl at 16 °C for 3 hours, according to the manufacturer's protocol (T4 DNA Ligase, New England BioLabs, NEB, Ipswich, MA). The whole fragments (634 bp) obtained from the ligation reaction were used as templates for a second PCR reaction, using the external U1-casup-FORNheI and U1-casdown-REVNheI primers. The reaction was performed in a final volume of 50 µl with a single series of 30 cycles, preceded by a 1 minute long predenaturation step, according to the above-mentioned protocol.

After amplification and purification, the resulting fragments were cloned in the forward orientation in the NheI site of a pAAV2.1-CMV-eGFP plasmid[32]: the total amount of PCR products and 10 µg of pAAV2.1-CMV-eGFP2 vector were

digested with NheI restriction enzyme (New England Bio-Labs, NEB) for 3 hours at 37 °C in a final volume of 50 µl. In order to prevent its potential recircularization, the restricted pAAV-2.1-CMV-eGFP vector was dephosphorylated by treatment with Calf Intestine Alkaline Phosphatase (CIAP, Fermentas, Thermo Fisher Scientific) at 37 °C for 30 minutes. The ligation reaction was performed at 16 °C for 3 hours in a final volume of 20 µl by using T4 DNA ligase (New England BioLabs, NEB). We confirmed the exact sequence and the orientation of the inserts within the pAAV-2.1CMV-eGFP vector by automated DNA sequencing (*BMR Genomics*, Padova), using the AAV Rev primer (**Table 2**).

Cell cultures and transfection. We transiently overexpressed wild type and mutant plasmids into African green monkey kidney cells (COS-1). COS-1 cells were cultured in Dulbecco's modified Eagles-Hams F10 medium (1:1 vol/vol) with fetal bovine serum (10%) and antibiotics (Penicillin-Streptomycin 1×) and grown in a humidified incubator, at 5% CO_2 and 37 °C.

Transfection of COS-1 cells was mediated by Lipofectamine LTX (Life Technologies, Carlsbad, CA) using a plasmid DNA/lipofectamine ratio of 1 µg: 3 µl. COS-1 cells were plated onto 6-multi well plates (7.5×10^5 cells/well). For each transfection an amount of 2.5 µg for reporter minigenes (size about 6.0 kb) and 1.25 µg for U1asRNA constructs (size about 6.0 kb) were used, to obtain a final molar ratio of 2:1. After 4 hours of incubation, the medium was replaced with fresh growth medium and cells were incubated for 48 hours before harvesting by trypsinization. After trypsinization, cells were washed once with Phosphate buffered saline (PBS) 1X and resuspended in water supplemented with a protease inhibitor (Sigma-Aldrich). Pellets were stored at –20 °C for protein analysis or at –80 °C for RNA analysis.

RNA isolation, retrotranscription, and reverse transcriptase-PCR (RT-PCR). Total RNA was isolated from transfected COS-1 cells using the RNeasy mini kit (Qiagen). RNA integrity and concentration were checked both by 1% agarose gel and Nanodrop ND-1000 Spectrophotometer (Nanodrop technologies, Wilmington).

Total RNA (200 ng) was reverse transcribed with random hexamers using TaqMan Reverse Transcriptase kit (Applied Biosystems by Life Technologies) as previously described.[4]

We performed RT-PCR analysis using 2 µl of retrotranscribed products as template and primers RNA3F and RNA5R that anneal on the *GLA* exons 3 and 5 respectively. This primer couple includes the region that differs between the two alternative *GLA* transcripts and produces an amplicon of 406 bp corresponding to the wild-type *GLA* mRNA and an amplicon of 463 bp from the GLAins57 transcript. PCR reactions were prepared in 25 µl of final volume in a reaction mixture containing 1X PCR buffer, 1.5 mmol/l MgCl2, 250 µmol/l each dNTP, 15 pmol of each primer, 1 U of *Taq* DNA polymerase (Applied Biosystems by Life Technologies). After a primary denaturation for 5 minutes at 95 °C, amplification was carried out for 30 cycles of 30 seconds at 95 °C, 30 seconds at 56 °C and 2 minutes at 72 °C, with a final extension of 7 minutes at 72 °C. Densitometric analysis was performed using ImageJ densitometry software (http://imagej.nih.gov/ij/). Densitometry values of RT-PCR replicates were expressed as mean ± SD.

Assessment of U1asRNA expression in transfected COS-1 cells. To verify the transcription of U1asRNAs from the vectors transfected in COS-1 cells, and confirm their integrity, we adapted the previously reported protocol by Denti *et al.*[29] RT-PCRs were carried out on retrotranscribed total RNA (2 µl corresponding to 10 ng of RNA) with primer U1+130,[29] which anneals on the body of the U1 mRNA molecule, in combination with a primer specific for the engineered antisense modified U1 tail. Primer pU1-GLA was used to amplify the transcript from U1-GLA3T, U1-WT and U1-GLA5A and primer pU1-Scramble for the amplification of the U1-GLAScramble RNA. PCR reactions were performed as described above for RT-PCR changing the annealing temperature to 54 °C. The U1asRNA amplification products have a length c.a. 100 bp.

Quantification of the GLA mRNA transcripts. We measured the *GLA* mRNA transcripts using a quantitative real-time RT-PCR method based on TaqMan technology and a Fast Real-Time PCR System (Applied Biosystems by Life Technologies). Probes, primers and protocols used were previously reported.[4] For the detection of the *GLA* mRNA that encodes α-Gal A: probe 631/666 nt, we used forward primer 579/602 nt and reverse primer 688/668 nt. For the detection of the GLAins57 mRNA, we used probe 670/701 nt, forward primer 642/668 nt and reverse primer 738/718 nt.

For the absolute quantification of *GLA* mRNA which encodes the lysosomal α-Gal A, we used the wild-type pCD-GLA plasmid[4] while for the GLAins57 mRNA, the following oligonucleotide was designed on the cDNA carrying the intronic insertion of 57 nt (1347 bp) and generated by Roche, Mannheim, Germany: oligonucleotide *GLA*mut 5′-CTCCACACTATTTGGAAGTATTTGTTGACTTGTTAC-CATGTCTCCCCACTAAAGTCCCAATTATACAGAAATC-CGACAGTACTGCAATCACTGGCGA-3′ (642/738 nt). The pCD-GLA plasmid and *GLA*mut oligonucleotide were serially diluted 10-fold from a starting quantity of 10^8 ag for the wild-type pCD-GLA and 10^7 ag for the *GLA*mut oligonucleotide and used as standard curves. The absolute values of *GLA* gene mRNA products were expressed as copy/mg of total RNA (mean ± SD).

Western blot assay. Transfected COS-1 cells were harvested by trypsin and cell pellets were frozen at –80 °C until assayed. Cell pellets were lysed in sterile distilled water containing complete protease inhibitor cocktail (BD Biosciences, Erembodegem, Belgium) by sonication (10 seconds). The protein concentration for each lysate was measured using the Micro BCA protein Assay kit (Pierce, Rockford, IL). Total protein (30 µg) from each lysate was loaded onto homemade 12.5% polyacrylamide gels containing 0.1% SDS and transferred onto nitrocellulose membranes (Bio-Rad, Hercules, CA) using the Mini Trans-Blot system (Bio-Rad). Immunoblots were then probed with a 1:200 dilution of rabbit polyclonal antibody for α-Gal A kindly provided by Genzyme Corporation (Genzyme, Italy) and a 1:2,500 dilution of rabbit polyclonal antibody for cyclophilin A (Millipore, Billerica, MA). Cyclophilin A was used as a loading control.[72,73] The blots were then incubated with secondary anti-rabbit IgG (whole molecule) conjugated to alkaline phosphatase (SIGMA; Milano, Italy), and signals were revealed using the AP Conjugate Substrate kit (Bio-Rad).

α-Gal A enzyme assay. α-Gal A enzyme assays were performed in triplicate by fluorogenic method[49] with the following modifications: 1 mg/ml cell lysates (diluted in 10 µl of heat inactivated 0.2% BSA+0.02% Na Azide) were added to 20 µl substrate (4-MU-a-D-galactopyranoside 5 mmol/l in 0.1 M Na-acetate buffer, pH 4.5 + 150 mmol/l N-acetyl-D-galactosamine and 0.02% Na Azide); stop solution: 200 µL of 0.5 M Na-HCO3-Na2CO3 buffer, pH 10.7, 0.025% Triton X-100. The Micro BCA protein Assay kit (Pierce) was used to set up the starting protein concentrations used in each enzyme assay performed in black 96-well microplates. Fluorescence was read on a Spectra Max M2 microplate Reader (Molecular Devices, Toronto, Canada).

Statistical analysis. We evaluated data for qPCR for statistical significance using the Student's *t*-test (GraphPad Software, San Diego, CA), expressed as mean ± SD ($n = 3$). A *P value of <0.05 was considered significant for data acquired in density units.

Gene variants nomenclature and reference sequences. Gene variants are given in the text by following the Human Genome Variation Society (HGVS) recommendations (http://www.hgvs.org/mutnomen/). Exon numbering refers to the *GLA* RefSeq NM_000169.2 (*GLA*; Gene ID 2717).

1. Zarate, YA and Hopkin, RJ (2008). Fabry's disease. *Lancet* **372**: 1427–1435.
2. Desnick, R, Ioannou, Y, and Eng, C (2001). α-Galactosidase a deficiency: Fabry disease. In: Scriver CR, Beaudet AL, Sly WS and Valle D (eds.). *The Metabolic and Molecular Bases of Inherited Disease*. 8th edn. McGraw-Hill: New York 2001: 3733–3774.
3. MacDermot, KD, Holmes, A and Miners, AH (2001). Anderson-Fabry disease: clinical manifestations and impact of disease in a cohort of 60 obligate carrier females. *J Med Genet* **38**: 769–775.
4. Filoni, C, Caciotti, A, Carraresi, L, Donati, MA, Mignani, R, Parini, R *et al.* (2008). Unbalanced GLA mRNAs ratio quantified by real-time PCR in Fabry patients' fibroblasts results in Fabry disease. *Eur J Hum Genet* **16**: 1311–1317.
5. Ishii, S, Nakao, S, Minamikawa-Tachino, R, Desnick, RJ and Fan, JQ (2002). Alternative splicing in the alpha-galactosidase A gene: increased exon inclusion results in the Fabry cardiac phenotype. *Am J Hum Genet* **70**: 994–1002.
6. Hsu, TR, Sung, SH, Chang, FP, Yang, CF, Liu, HC, Lin, HY *et al.* (2014). Endomyocardial biopsies in patients with left ventricular hypertrophy and a common Chinese later-onset Fabry mutation (IVS4 + 919G > A). *Orphanet J Rare Dis* **9**: 96.
7. Lin, HY, Chong, KW, Hsu, JH, Yu, HC, Shih, CC, Huang, CH *et al.* (2009). High incidence of the cardiac variant of Fabry disease revealed by newborn screening in the Taiwan Chinese population. *Circ Cardiovasc Genet* **2**: 450–456.
8. Hwu, WL, Chien, YH, Lee, NC, Chiang, SC, Dobrovolny, R, Huang, AC *et al.* (2009). Newborn screening for Fabry disease in Taiwan reveals a high incidence of the later-onset GLA mutation c.936+919G>A (IVS4+919G>A). *Hum Mutat* **30**: 1397–1405.
9. Arechavala-Gomeza, V, Khoo, B and Aartsma-Rus, A (2014). Splicing modulation therapy in the treatment of genetic diseases. *Appl Clin Genet* **7**: 245–252.
10. Bacchi, N, Casarosa, S and Denti, MA (2014). Splicing-correcting therapeutic approaches for retinal dystrophies: where endogenous gene regulation and specificity matter. *Invest Ophthalmol Vis Sci* **55**: 3285–3294.
11. Siva, K, Covello, G and Denti, MA (2014). Exon-skipping antisense oligonucleotides to correct missplicing in neurogenetic diseases. *Nucleic Acid Ther* **24**: 69–86.

12. Veltrop, M and Aartsma-Rus, A (2014). Antisense-mediated exon skipping: taking advantage of a trick from Mother Nature to treat rare genetic diseases. *Exp Cell Res* **325**: 50–55.
13. Turczynski, S, Titeux, M, Pironon, N and Hovnanian, A (2012). Antisense-mediated exon skipping to reframe transcripts. *Methods Mol Biol* **867**: 221–238.
14. Aartsma-Rus, A (2012). Overview on DMD exon skipping. *Methods Mol Biol* **867**: 97–116.
15. Goyenvalle, A (2012). Engineering U7snRNA gene to reframe transcripts. *Methods Mol Biol* **867**: 259–271.
16. Martone, J, De Angelis, FG and Bozzoni, I (2012). U1 snRNA as an effective vector for stable expression of antisense molecules and for the inhibition of the splicing reaction. *Methods Mol Biol* **867**: 239–257.
17. Nlend, RN and Schümperli, D (2012). Antisense genes to induce exon inclusion. *Methods Mol Biol* **867**: 325–347.
18. Gorman, L, Suter, D, Emerick, V, Schümperli, D and Kole, R (1998). Stable alteration of pre-mRNA splicing patterns by modified U7 small nuclear RNAs. *Proc Natl Acad Sci USA* **95**: 4929–4934.
19. Suter, D, Tomasini, R, Reber, U, Gorman, L, Kole, R and Schümperli, D (1999). Double-target antisense U7 snRNAs promote efficient skipping of an aberrant exon in three human beta-thalassemic mutations. *Hum Mol Genet* **8**: 2415–2423.
20. Guiro, J and O'Reilly, D (2015). Insights into the U1 small nuclear ribonucleoprotein complex superfamily. *Wiley Interdiscip Rev RNA* **6**: 79–92.
21. Schümperli, D and Pillai, RS (2004). The special Sm core structure of the U7 snRNP: far-reaching significance of a small nuclear ribonucleoprotein. *Cell Mol Life Sci* **61**: 2560–2570.
22. Denti, MA, Rosa, A, Sthandier, O, De Angelis, FG and Bozzoni, I (2004). A new vector, based on the PolII promoter of the U1 snRNA gene, for the expression of siRNAs in mammalian cells. *Mol Ther* **10**: 191–199.
23. Benchaouir, R, Meregalli, M, Farini, A, D'Antona, G, Belicchi, M, Goyenvalle, A *et al.* (2007). Restoration of human dystrophin following transplantation of exon-skipping-engineered DMD patient stem cells into dystrophic mice. *Cell Stem Cell* **1**: 646–657.
24. De Angelis, FG, Sthandier, O, Berarducci, B, Toso, S, Galluzzi, G, Ricci, E *et al.* (2002). Chimeric snRNA molecules carrying antisense sequences against the splice junctions of exon 51 of the dystrophin pre-mRNA induce exon skipping and restoration of a dystrophin synthesis in Delta 48-50 DMD cells. *Proc Natl Acad Sci USA* **99**: 9456–9461.
25. Hartmann, L, Neveling, K, Borkens, S, Schneider, H, Freund, M, Grassman, E *et al.* (2010). Correct mRNA processing at a mutant TT splice donor in FANCC ameliorates the clinical phenotype in patients and is enhanced by delivery of suppressor U1 snRNAs. *Am J Hum Genet* **87**: 480–493.
26. Vacek, MM, Ma, H, Gemignani, F, Lacerra, G, Kafri, T and Kole, R (2003). High-level expression of hemoglobin A in human thalassemic erythroid progenitor cells following lentiviral vector delivery of an antisense snRNA. *Blood* **101**: 104–111.
27. Denti, MA, Incitti, T, Sthandier, O, Nicoletti, C, De Angelis, FG, Rizzuto, E *et al.* (2008). Long-term benefit of adeno-associated virus/antisense-mediated exon skipping in dystrophic mice. *Hum Gene Ther* **19**: 601–608.
28. Denti, MA, Rosa, A, D'Antona, G, Sthandier, O, De Angelis, FG, Nicoletti, C *et al.* (2006). Chimeric adeno-associated virus/antisense U1 small nuclear RNA effectively rescues dystrophin synthesis and muscle function by local treatment of mdx mice. *Hum Gene Ther* **17**: 565–574.
29. Denti, MA, Rosa, A, D'Antona, G, Sthandier, O, De Angelis, FG, Nicoletti, C *et al.* (2006). Body-wide gene therapy of Duchenne muscular dystrophy in the mdx mouse model. *Proc Natl Acad Sci USA* **103**: 3758–3763.
30. Goyenvalle, A, Vulin, A, Fougerousse, F, Leturcq, F, Kaplan, JC, Garcia, L *et al.* (2004). Rescue of dystrophic muscle through U7 snRNA-mediated exon skipping. *Science* **306**: 1796–1799.
31. Incitti, T, De Angelis, FG, Cazzella, V, Sthandier, O, Pinnarò, C, Legnini, I *et al.* (2010). Exon skipping and duchenne muscular dystrophy therapy: selection of the most active U1 snRNA antisense able to induce dystrophin exon 51 skipping. *Mol Ther* **18**: 1675–1682.
32. Auricchio, A, Kobinger, G, Anand, V, Hildinger, M, O'Connor, E, Maguire, AM *et al.* (2001). Exchange of surface proteins impacts on viral vector cellular specificity and transduction characteristics: the retina as a model. *Hum Mol Genet* **10**: 3075–3081.
33. Desnick, RJ (2004). Enzyme replacement therapy for Fabry disease: lessons from two alpha-galactosidase A orphan products and one FDA approval. *Expert Opin Biol Ther* **4**: 1167–1176.
34. Buechner, S, Moretti, M, Burlina, AP, Cei, G, Manara, R, Ricci, R *et al.* (2008). Central nervous system involvement in Anderson-Fabry disease: a clinical and MRI retrospective study. *J Neurol Neurosurg Psychiatry* **79**: 1249–1254.
35. Jardim, LB, Aesse, F, Vedolin, LM, Pitta-Pinheiro, C, Marconato, J, Burin, MG *et al.* (2006). White matter lesions in Fabry disease before and after enzyme replacement therapy: a 2-year follow-up. *Arq Neuropsiquiatr* **64**(3B): 711–717.
36. Rombach, SM, Smid, BE, Bouwman, MG, Linthorst, GE, Dijkgraaf, MG and Hollak, CE (2013). Long term enzyme replacement therapy for Fabry disease: effectiveness on kidney, heart and brain. *Orphanet J Rare Dis* **8**: 47.
37. Rombach, SM, Smid, BE, Linthorst, GE, Dijkgraaf, MG and Hollak, CE (2014). Natural course of Fabry disease and the effectiveness of enzyme replacement therapy: a systematic review and meta-analysis: effectiveness of ERT in different disease stages. *J Inherit Metab Dis* **37**: 341–352.
38. Deegan, PB (2012). Fabry disease, enzyme replacement therapy and the significance of antibody responses. *J Inherit Metab Dis* **35**: 227–243.

39. Ferri, L, Guido, C, la Marca, G, Malvagia, S, Cavicchi, C, Fiumara, A *et al.* (2012). Fabry disease: polymorphic haplotypes and a novel missense mutation in the GLA gene. *Clin Genet* **81**: 224–233.

40. Filoni, C, Caciotti, A, Carraresi, L, Cavicchi, C, Parini, R, Antuzzi, D *et al.* (2010). Functional studies of new GLA gene mutations leading to conformational Fabry disease. *Biochim Biophys Acta* **1802**: 247–252.

41. Wu, X, Katz, E, Della Valle, MC, Mascioli, K, Flanagan, JJ, Castelli, JP *et al.* (2011). A pharmacogenetic approach to identify mutant forms of α-galactosidase A that respond to a pharmacological chaperone for Fabry disease. *Hum Mutat* **32**: 965–977.

42. Germain, DP, Giugliani, R, Hughes, DA, Mehta, A, Nicholls, K, Barisoni, L *et al.* (2012). Safety and pharmacodynamic effects of a pharmacological chaperone on α-galactosidase A activity and globotriaosylceramide clearance in Fabry disease: report from two phase 2 clinical studies. *Orphanet J Rare Dis* **7**: 91.

43. Warnock, DG, Bichet, DG, Holida, M, Goker-Alpan, O, Nicholls, K, Thomas, M *et al.* (2015). Oral Migalastat HCl Leads to Greater Systemic Exposure and Tissue Levels of Active α-Galactosidase A in Fabry Patients when Co-Administered with Infused Agalsidase. *PLoS One* **10**: e0134341.

44. Garman, SC (2007). Structure-function relationships in alpha-galactosidase A. *Acta Paediatr* **96**: 6–16.

45. Garman, SC and Garboczi, DN (2004). The molecular defect leading to Fabry disease: structure of human alpha-galactosidase. *J Mol Biol* **337**: 319–335.

46. Ishii, S, Chang, HH, Kawasaki, K, Yasuda, K, Wu, HL, Garman, SC *et al.* (2007). Mutant alpha-galactosidase A enzymes identified in Fabry disease patients with residual enzyme activity: biochemical characterization and restoration of normal intracellular processing by 1-deoxygalactonojirimycin. *Biochem J* **406**: 285–295.

47. Sugawara, K, Tajima, Y, Kawashima, I, Tsukimura, T, Saito, S, Ohno, K *et al.* (2009). Molecular interaction of imino sugars with human alpha-galactosidase: Insight into the mechanism of complex formation and pharmacological chaperone action in Fabry disease. *Mol Genet Metab* **96**: 233–238.

48. Yam, GH, Bosshard, N, Zuber, C, Steinmann, B and Roth, J (2006). Pharmacological chaperone corrects lysosomal storage in Fabry disease caused by trafficking-incompetent variants. *Am J Physiol Cell Physiol* **290**: C1076–C1082.

49. Benjamin, ER, Flanagan, JJ, Schilling, A, Chang, HH, Agarwal, L, Katz, E *et al.* (2009). The pharmacological chaperone 1-deoxygalactonojirimycin increases alpha-galactosidase A levels in Fabry patient cell lines. *J Inherit Metab Dis* **32**: 424–440.

50. Germain, DP and Fan, JQ (2009). Pharmacological chaperone therapy by active-site-specific chaperones in Fabry disease: *in vitro* and preclinical studies. *Int J Clin Pharmacol Ther* **47 Suppl 1**: S111–S117.

51. Inagaki, K, Fuess, S, Storm, TA, Gibson, GA, Mctiernan, CF, Kay, MA *et al.* (2006). Robust systemic transduction with AAV9 vectors in mice: efficient global cardiac gene transfer superior to that of AAV8. *Mol Ther* **14**: 45–53.

52. Trollet, C, Athanasopoulos, T, Popplewell, L, Malerba, A and Dickson, G (2009). Gene therapy for muscular dystrophy: current progress and future prospects. *Expert Opin Biol Ther* **9**: 849–866.

53. Zincarelli, C, Soltys, S, Rengo, G and Rabinowitz, JE (2008). Analysis of AAV serotypes 1-9 mediated gene expression and tropism in mice after systemic injection. *Mol Ther* **16**: 1073–1080.

54. Xiong, HY, Alipanahi, B, Lee, LJ, Bretschneider, H, Merico, D, Yuen, RK *et al.* (2015). RNA splicing. The human splicing code reveals new insights into the genetic determinants of disease. *Science* **347**: 1254806.

55. Curado, J, Iannone, C, Tilgner, H, Valcárcel, J and Guigó, R (2015). Promoter-like epigenetic signatures in exons displaying cell type-specific splicing. *Genome Biol* **16**: 236.

56. Smith, SA and Lynch, KW (2014). Cell-based splicing of minigenes. *Methods Mol Biol* **1126**: 243–255.

57. Desviat, LR, Pérez, B and Ugarte, M (2012). Minigenes to confirm exon skipping mutations. *Methods Mol Biol* **867**: 37–47.

58. Gaildrat, P, Killian, A, Martins, A, Tournier, I, Frébourg, T and Tosi, M (2010). Use of splicing reporter minigene assay to evaluate the effect on splicing of unclassified genetic variants. *Methods Mol Biol* **653**: 249–257.

59. Germain, DP (2010). Fabry disease. *Orphanet J Rare Dis* **5**: 30.

60. Mehta, A, Beck, M, Eyskens, F, Feliciani, C, Kantola, I, Ramaswami, U *et al.* (2010). Fabry disease: a review of current management strategies. *QJM* **103**: 641–659.

61. Schiffmann, R, Warnock, DG, Banikazemi, M, Bultas, J, Linthorst, GE, Packman, S *et al.* (2009). Fabry disease: progression of nephropathy, and prevalence of cardiac and cerebrovascular events before enzyme replacement therapy. *Nephrol Dial Transplant* **24**: 2102–2111.

62. Mignani, R, Feriozzi, S, Pisani, A, Cioni, A, Comotti, C, Cossu, M *et al.* (2008). Agalsidase therapy in patients with Fabry disease on renal replacement therapy: a nationwide study in Italy. *Nephrol Dial Transplant* **23**: 1628–1635.

63. Keslová-Veselíková, J, Hůlková, H, Dobrovolný, R, Asfaw, B, Poupetová, H, Berná, L *et al.* (2008). Replacement of alpha-galactosidase A in Fabry disease: effect on fibroblast cultures compared with biopsied tissues of treated patients. *Virchows Arch* **452**: 651–665.

64. Schiffmann, R, Rapkiewicz, A, Abu-Asab, M, Ries, M, Askari, H, Tsokos, M *et al.* (2006). Pathological findings in a patient with Fabry disease who died after 2.5 years of enzyme replacement. *Virchows Arch* **448**: 337–343.

65. Wu, Z, Asokan, A and Samulski, RJ (2006). Adeno-associated virus serotypes: vector toolkit for human gene therapy. *Mol Ther* **14**: 316–327.

66. Wang, G, Young, SP, Bali, D, Hutt, J, Li, S, Benson, J *et al.* (2014). Assessment of toxicity and biodistribution of recombinant AAV8 vector-mediated immunomodulatory gene therapy in mice with Pompe disease. *Mol Ther Methods Clin Dev* **1**: 14018.

67. Zacchigna, S, Zentilin, L and Giacca, M (2014). Adeno-associated virus vectors as therapeutic and investigational tools in the cardiovascular system. *Circ Res* **114**: 1827–1846.

68. Murrey, DA, Naughton, BJ, Duncan, FJ, Meadows, AS, Ware, TA, Campbell, KJ *et al.* (2014). Feasibility and safety of systemic rAAV9-hNAGLU delivery for treating mucopolysaccharidosis IIIB: toxicology, biodistribution, and immunological assessments in primates. *Hum Gene Ther Clin Dev* **25**: 72–84.

69. Nathwani, AC, Reiss, UM, Tuddenham, EG, Rosales, C, Chowdary, P, McIntosh, J *et al.* (2014). Long-term safety and efficacy of factor IX gene therapy in hemophilia B. *N Engl J Med* **371**: 1994–2004.

70. Buchholz, CJ, Friedel, T and Büning, H (2015). Surface-engineered viral vectors for selective and cell type-specific gene delivery. *Trends Biotechnol* **33**: 777–790.

71. Linthorst, GE, Hollak, CE, Donker-Koopman, WE, Strijland, A and Aerts, JM (2004). Enzyme therapy for Fabry disease: neutralizing antibodies toward agalsidase alpha and beta. *Kidney Int* **66**: 1589–1595.

72. Benjamin, ER, Khanna, R, Schilling, A, Flanagan, JJ, Pellegrino, LJ, Brignol, N *et al.* (2012). Co-administration with the pharmacological chaperone AT1001 increases recombinant human α-galactosidase A tissue uptake and improves substrate reduction in Fabry mice. *Mol Ther* **20**: 717–726.

73. Xu, S, Lun, Y, Brignol, N, Hamler, R, Schilling, A, Frascella, M *et al.* (2015). Coformulation of a novel human α-galactosidase A with the pharmacological chaperone AT1001 leads to improved substrate reduction in Fabry mice. *Mol Ther* **23**: 1169–1181.